EPJ Photovoltaics **15**, 24 (2024)

https://doi.org/10.1051/epjpv/2024007

Available online at:
www.epj-pv.org

Special Issue on 'EU PVSEC 2023: State of the Art and Developments in Photovoltaics', edited by Robert Kenny and João Serra

ORIGINAL ARTICLE

OPEN ACCESS

New approaches to edge passivation of laser cut PERC solar cells

Akash Thukaram[1,2,*], Dominik Rudolph[1], Andreas Halm[1], and Daniel Tune[1]

[1] International Solar Energy Research Center (ISC) Konstanz, Rudolf-Diesel-Str. 15, 78467 Konstanz, Germany
[2] halm elektronik gmbh, Friesstraße 20, 60388 Frankfurt am Main, Germany

Received: 16 July 2023 / Accepted: 18 January 2024

Abstract. Recently the development trend in the PV industry is towards much larger wafer formats. With increasing wafer area and the resulting increase in short-circuit current at the cell level, there is also a trend towards sub-cells (solar cell cut into smaller pieces) for module integration. Using sub-cells, the resistance losses through the connection can be reduced. Modules based on sub-cells achieve higher levels of fill factors and thus a higher nominal power. However, the energy yield of such sub-cells is reduced compared to full cells due to the non-passivated laser edge. The laser cut edge causes a high recombination of the charge carriers, which negatively affects the pseudo fill factor as well as open-circuit voltage of the cell. The current work introduces two different approaches for passivating the laser separated PERC solar cells. The experiments were performed on p-type PERC monofacial cells and laser scribe and mechanical cleavage (LSMC) technique was used to obtain sub-cells from the host cells. The method 'laser scribing and simultaneous Al doping' increases the pFF of the cleaved cells by $+0.2$–$0.4\%_{\text{abs}}$ in comparison to the reference cleaved cells whereas the method 'laser scribing and subsequent Al doping' shows an improvement in efficiency of the cleaved cells by $+0.2\%_{\text{abs}}$.

Keywords: PERC / laser scribe and mechanical cleavage (LSMC) / edge recombination

1 Introduction

According to the 2023 ITRPV roadmap, most of the silicon solar cells produced in 2022 were of M10 size with around 45% market share while M6 format contributed to around 28% share. The wafer formats below M6 are losing their market share. By 2033, M10 and G12 formats are expected to be dominating the market [1]. But with the increase in wafer area, there is an increase in the short circuit current at the cell level. Hence, the concept of laser-cut sub-cells is becoming more popular since the current-induced resistive power losses through the interconnectors can be minimized [2]. Modules based on sub-cells thus achieve higher output power densities and fill factors [3]. However, the energy yield of such sub-cells is decreased in comparison to the full cells due to an increased recombination current at the non-passivated laser-cut edge [4]. The losses at the edges have a significant impact on the solar cell performance, particularly for high efficiency solar cells such as modern passivated emitter and rear cells (PERC), interdigitated back contact (IBC) cells, cells with tunnel oxide passivated contacts (TOPCon) or hetero junction cells (HJT) [5].

There are different laser cutting technologies to produce half-cells, sub-cells and shingle stripes. One of them is the laser scribing and mechanical cleavage (LSMC) technique, where a pulsed laser beam is used to produce a predetermined breaking line on the cell. Later the cell is cleaved by mechanical breakage [6]. Apart from this, there are other techniques like laser induced cutting [7], thermal laser separation [8], laser microjet separation [9] and laser induced subsurface modification [10]. The common issue with all the processes is that the cut edge is not passivated which therefore leads to a high recombination of the charge carriers at the edges and negatively affects the pseudo fill factor and also the open-circuit voltage of the cell [11].

Edge losses in silicon solar cells is a major concern in the current photovoltaic research, especially while producing shingles which have high perimeter to area ratios. Various methods have been investigated in the past to reduce the edge recombination. The concept of edge surface field is introduced in reference [12], where the separation path is passivated by heavy doping. This heavily doped edge region creates an electric field that repels the carriers and minimizes recombination at the cut edges. It has been reported in reference [13] that a passivation effect can be seen when the edge is wet chemically treated as there is a thermal growth of SiO_2 on the edge. Baliozian et al. introduced the PET (passivated edge technology) process

* e-mail: akash.bhushan6@gmail.com

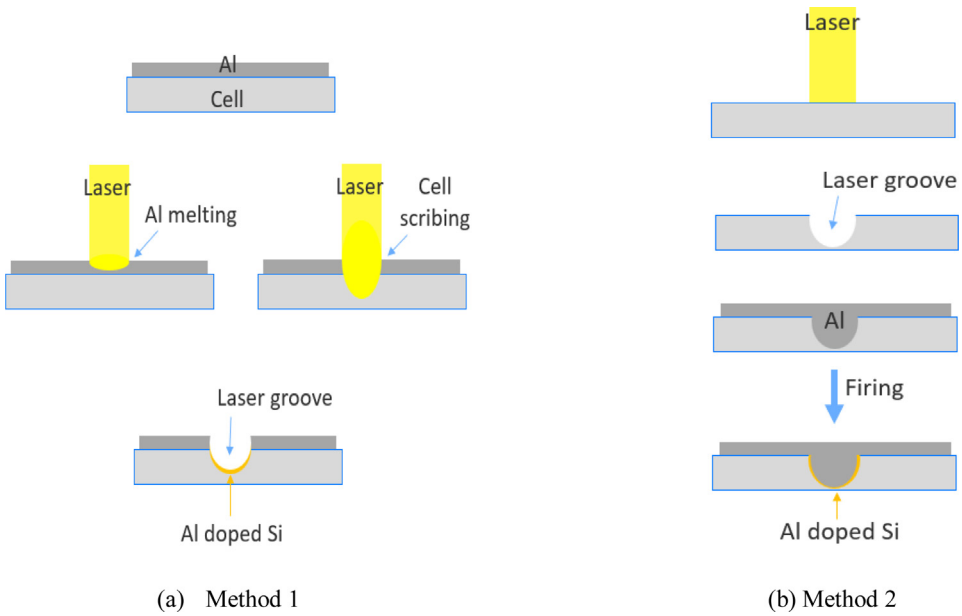

Fig. 1. Experimental steps of (a) method 1 and (b) method 2.

Table 1. Laser parameters for aluminium melting with the high-powered infrared laser.

Set	Pulse repetition rate (kHz) f_{rep}	Speed v (mm/s)	Pulse overlap (%)	Pump power (%)	Measured spot diameter (μm)	Repetitions
1	20	96	95	60	96	0
2	20	960	50	60	96	0
3	50	180	95	60	72	0
4	50	1800	50	60	72	0
5	80	240	95	60	60	0
6	80	2400	50	60	60	0
7	80	240	95	60	60	10
8	80	2400	50	60	60	10

for passivating the edges of separated solar cells, which consists of deposition of aluminium oxide followed by annealing [14]. Daniel et al. investigated on edge passivation by treatment with the organic fluoropolymer Nafion [15]. There was also another experiment in which PET sequence was applied to TOPCon shingle solar cells produced using the TLS laser technique [16]. Münzer et al. introduced post separation edge passivation technique for silicon heterojunction (SHJ) half solar cells which were separated using thermal laser separation [17]. Optimization paths to reduce cutting induced degradations losses from laser cutting process were introduced by Gerenton et al. for SHJ solar cells to improve the cell performance [18].

This article introduces two different approaches for passivating the LSMC treated PERC solar cells. The experiments were performed on p-type PERC cells. The main goal of the work is to passivate the laser cut edges and examine if there are improvements in the cell's IV parameters. The reproducibility of the process is evaluated, as well as whether it can be easily implemented in cell production lines.

2 Experimental

2.1 Laser scribing and simultaneous Al doping

The aim of this method is to develop a process in which the cell is cut using a laser process and the edge is simultaneously doped with aluminium. Figure 1a illustrates the experimental procedure of this method. The finished p-type G1 PERC monofacial cells with aluminium printed on the rear side were laser processed using a high-powered infrared laser in two steps, both carried out successively. The first laser process used the parameters specified in Table 1, which melted the aluminium while the second laser process used the standard cutting recipe for scribing the cells on the rear side. Eight different variations

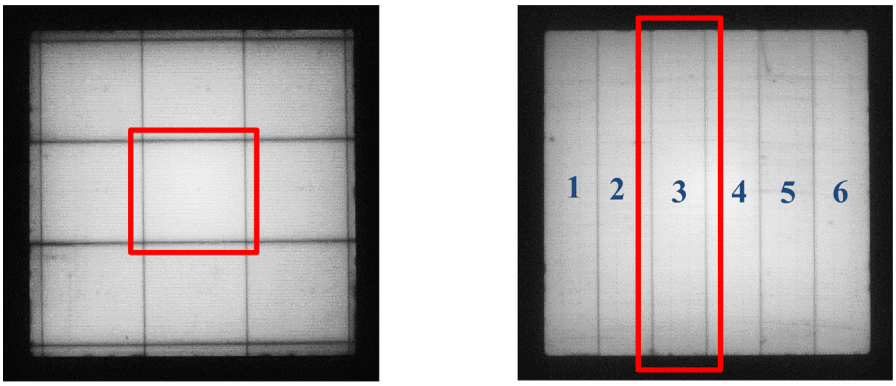

(a) (b)

Fig. 2. PL images of the cell (a) scribed into nine square parts, (b) scribed into six parts.

Table 2. Different groups with their variation in laser scribing.

Group	Cell number	Type of laser processing
G1	9, 10, 11, 12	Standard – single scribe
G3	1, 2, 3, 4	Two scribes with 20 µm offset
Reference	5, 6, 7, 8	No laser processing

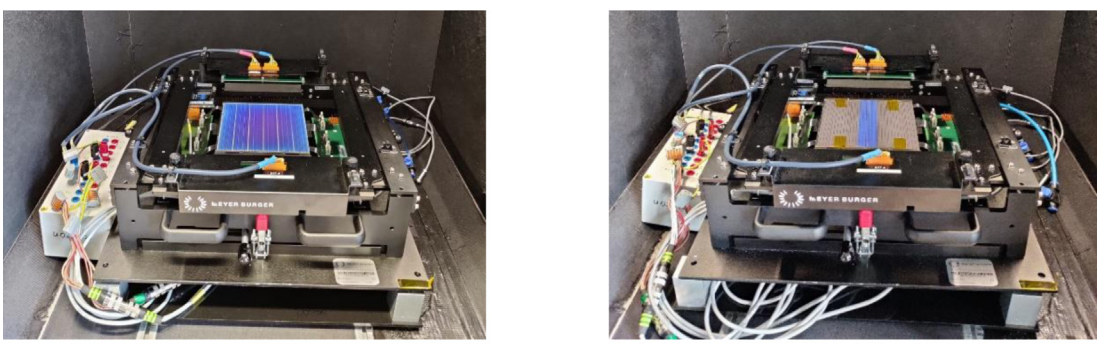

(a) (b)

Fig. 3. Grid touch setup for (a) full cell, (b) cleaved cell.

of the laser parameters for melting the aluminium were chosen and were grouped into eight sets. Each set consists of two cells. Each cell was scribed into nine parts in order to produce sub-cells with dimensions 50 mm × 50 mm, shown in Figure 2a. A reference cell which was only laser-scribed into nine parts using the standard cutting recipe was used for comparison.

2.2 Laser scribing and subsequent Al doping

This method also aims to dope the laser-cut edges of the cell with aluminium as in the previous method. Figure 1b shows the experimental steps of this method. Here the cells were laser scribed on the rear side prior to metallization using the high-powered infrared laser and then metallized by screen printing, followed by firing. Different variations of the standard recipe were used to scribe the cells in order to vary the width and the depth of the cut, separated into different groups. Table 2 shows the different groups along with their type of laser processing. The cells with no laser scribing before metallization, which followed the standard processing steps, were used as reference cells. Six sub-cells were obtained from laser scribing of one host wafer, each exhibiting dimensions of 158.75 mm × 26.46 mm, shown in Figure 2b.

3 Characterization

The IV parameters of the cells were measured using a xenon flasher sun simulator using the grid touch setup. Figures 3a and 3b show the grid touch setup for full cells as well as cleaved cells respectively. Here, the cells were contacted with the strings of the setup perpendicular to the fingers of the cells. The contacting of the fingers leads to the underestimation of series resistance losses, since the current

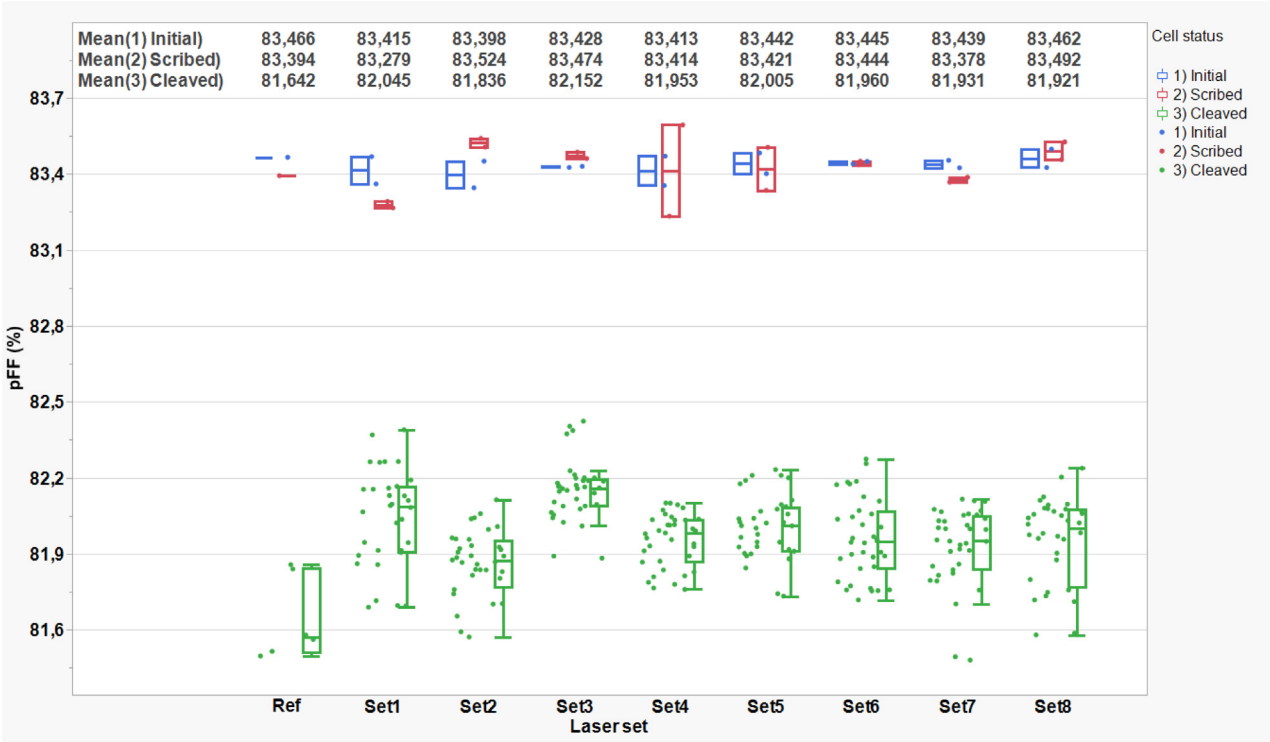

(a)

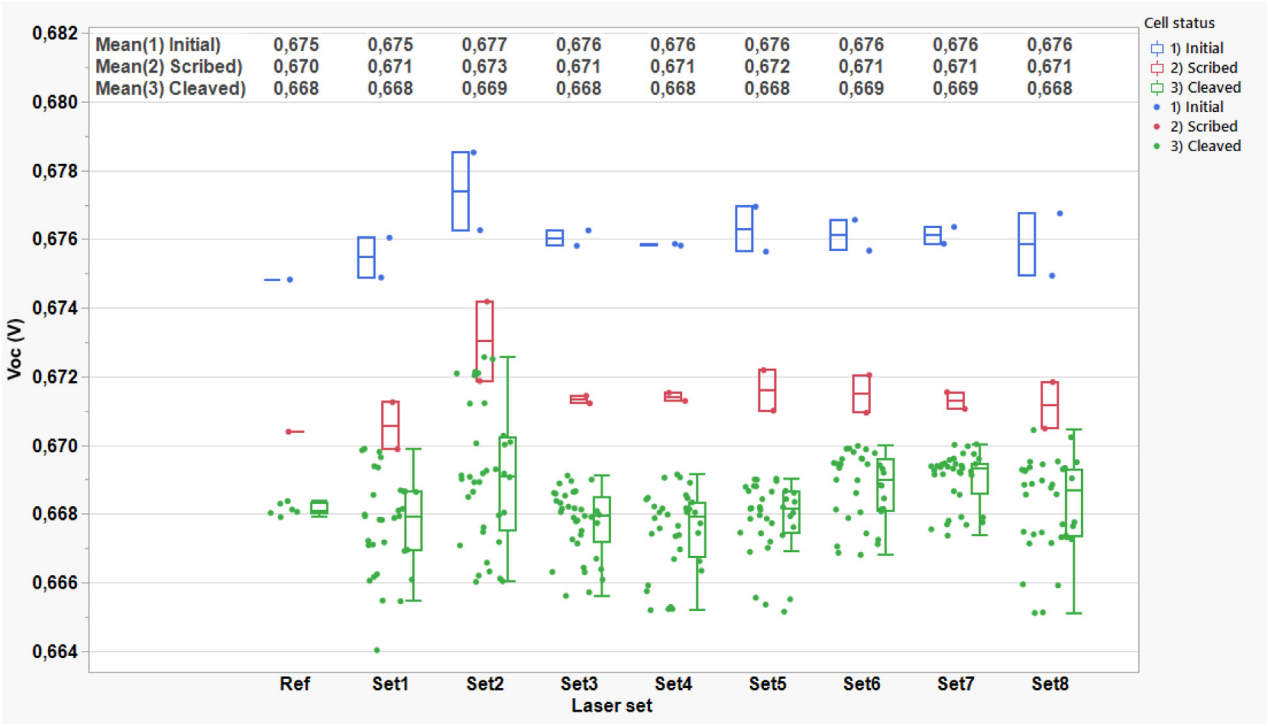

(b)

Fig. 4. (a) pFF values, (b) V_{OC} values and (c) η values attained by I–V measurements of the cells at initial, scribed and cleaved states.

(c)

Fig. 4. (Continued).

paths are reduced by the strings contacting of the grid touch [19]. The parameters such as pseudo fill factor (pFF), open-circuit voltage (V_{OC}), short-circuit current density (J_{SC}) and efficiency (η) were measured at room temperature (25 °C) and at 1000 W/m^2 illumination intensity. These parameters were compared at initial, laser scribed and cleaved states. From the photoluminescence (PL) imaging tool, high resolution PL images of the cells could be acquired at a current of 28.8 A and an integration time of 3 s, which corresponds to 1 sun illumination. These images were used to compare the intensities of the untreated edges with treated edges. The cleaved samples were measured using a macro lens. The samples were illuminated using two 30-W cw diode lasers with the wavelength of 808 nm. The images were acquired using a peltier cooled Si-CCD camera with gallium arsenide (GaAs) filter and resolution up to 1024×1024 pixels. The intensity graphs from the PL images were plotted using ImageJ software. In addition, the roughness, height, width as well as depth of the laser groove were measured using the laser scanning microscopy (LSM) by Olympus. Also, the quality of the edge doping with aluminium was evaluated using this tool. The LSM images of the treated edges were compared with those of the untreated edges.

4 Results and discussion

4.1 Result analysis of laser scribing and simultaneous Al doping

The pFF comparison of the cells at initial, laser scribed and cleaved states is shown in Figure 4a. Initially, the cells from all the sets including the reference cell have a pFF of approximately 83.4%. There is no significant difference observed after scribing these cells. However, there is a considerable decrease in the values after the cells are cleaved. Compared to the reference cleaved cells, all the cleaved cells from other sets which have some aluminium melting show a higher value. The pFF of the reference cleaved cells is around 81.6% while those from other sets have values ranging from 81.8% to 82%. Figure 4b shows the V_{OC} comparison of the cells at all the three stages. In terms of cleaved state, reference cells as well as the cells from other sets show similar values. The efficiency comparison of the cells at three different stages is shown in Figure 4c. There is drop in the values at each stage. At initial stage, the efficiency of the cells is around 22%, after scribing the efficiency drops to almost 21.6%. There is a further reduction in the efficiency after breaking the cells. The reference cleaved cells have an efficiency of around 21.43% whereas cells from other sets have slightly higher values compared to reference. Set 3 has the highest value of efficiency of around 21.53%. Also, significant difference between the initial and scribed state is seen in V_{OC} and efficiency compared to pFF, which shows no difference. The treated cells also show significantly higher scattering (standard deviation is larger) for V_{OC} and efficiency compared to the reference set. No considerable difference could be observed in terms of J_{SC} with regard to cleaved state.

The PL images of the cleaved reference cell and cells from other sets were taken at 1 sun illumination and intensity graphs (graph showing the intensity difference of the PL image plotted along the point of interest – here the yellow arrow line) were plotted along the direction shown

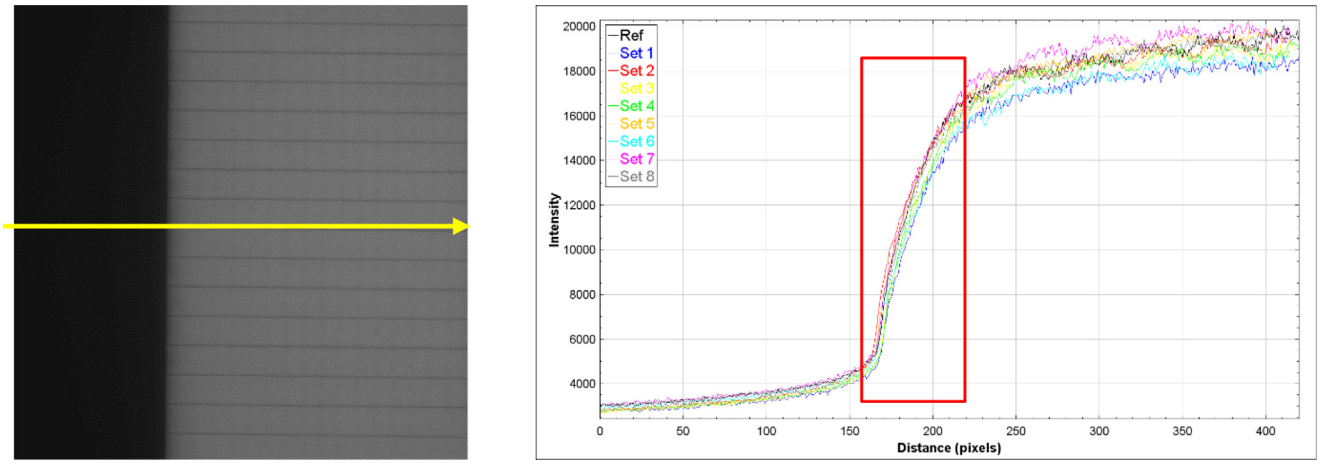

Fig. 5. PL image of the cleaved cell from set 1 under 1-sun illumination, along with the intensity graph of all sets.

in Figure 5. The small cell in the center of the whole big cell, marked in red in Figure 2a were used for result analysis. The steepness of the intensity curves was examined by calculating their slopes, which is shown in Figure 6. The slope values for each set were calculated for the section of the respective curve defined within the red box shown in Figure 5. The slopes of all treated laser sets are higher in comparison to the reference. However, set 3 shows the highest value.

From the results of the above experiment, it can be concluded that cells which had aluminium melting on the edges performed better than the cells with no edge treatment (which was taken as the reference cell). There was an improvement in some of the electrical parameters of the cells which had Al melting compared to the reference. In terms of pFF, there was a drop of 1.8% (ΔpFF = − 1.8%) from the host wafer to the separated state for the reference cell. Although the cleaved cells from all the sets showed some increase in the pFF compared to the reference cleaved cells, set 3 showed a highest value reaching ΔpFF = +0.4%. There was slight gain in the efficiency of the cells from all the sets in comparison to the reference cells. Set 3 had an increase of $\Delta\eta$ = +0.1%. The results from PL imaging also supported the results shown in IV measurements, with set 3 performing better than other sets and the reference. In conclusion, this method could show an edge passivation effect; however, a larger effect was seen from set 3, which had laser cutting speed of 180 mm/s, pulse repetition rate of 50 kHz, pump power of 60% and pulse overlap of 95%.

4.2 Result analysis of laser scribing and subsequent Al doping

V_{OC} comparison of all the cells from method 2 is shown in Figure 7a. The initial V_{OC} values of the reference cells are around 676 mV. With regard to the scribed state, group 3 shows a slightly lower value compared to the reference group and group 1. For the cleaved state, group 1 cells show a higher value in comparison to the reference group and group 3, which both show comparable values. For both laser-treated groups 1 and 3, the difference in V_{OC} between

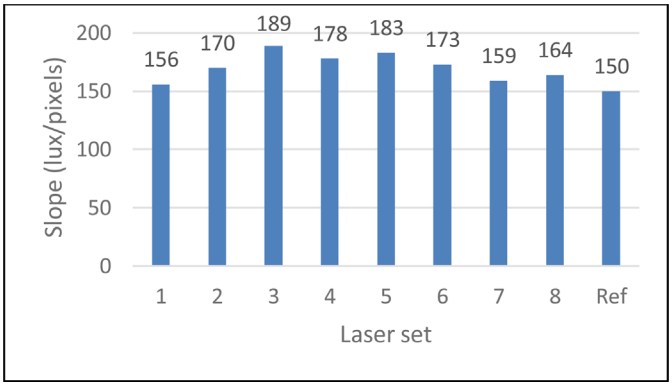

Fig. 6. Slope values for different sets at 1 sun illumination.

the scribed and cleaved states is around 2 to 3 mV, while for the reference this difference is around 4 − 5 mV. Hence the reference group clearly suffers more strongly due to the cell cleavage than the two laser-treated groups. The comparison of the efficiencies of the cells from method 2 is shown in Figure 6b. The efficiency of the reference cells is initially around 22%. The difference between efficiency values of scribed cells from group 1 and the reference group is very little, while group 3 shows a slight decrease in values. For the cleaved state, group 1 shows higher values of efficiency compared to group 3 and the reference group. No significant difference was observed in terms of pFF and J_{SC} values between the cleaved reference cells and cells from other groups.

The PL images of the cleaved cells from the reference group and other groups were taken at 1 sun and their intensity graphs were plotted along the direction shown in Figure 8. Cell number 3 (marking shown in Fig. 2b) of the reference, group 1 and group 3 were used for result analysis. Figure 9 shows the slope of the curves from different groups at 1 sun. Group 1 and Group 3 show a higher value of the slope compared to the reference. Yet, group 1 shows the highest value. Hence these results support the results of IV measurements, with group 1 showing a better performance mainly in terms of efficiency.

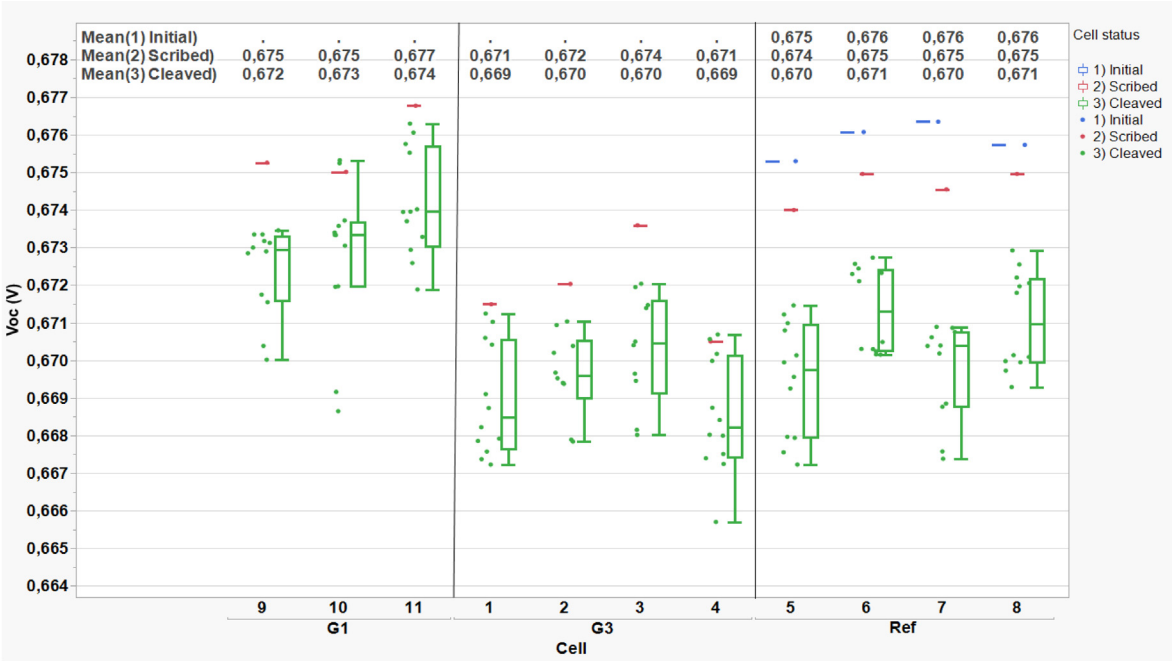

(a)

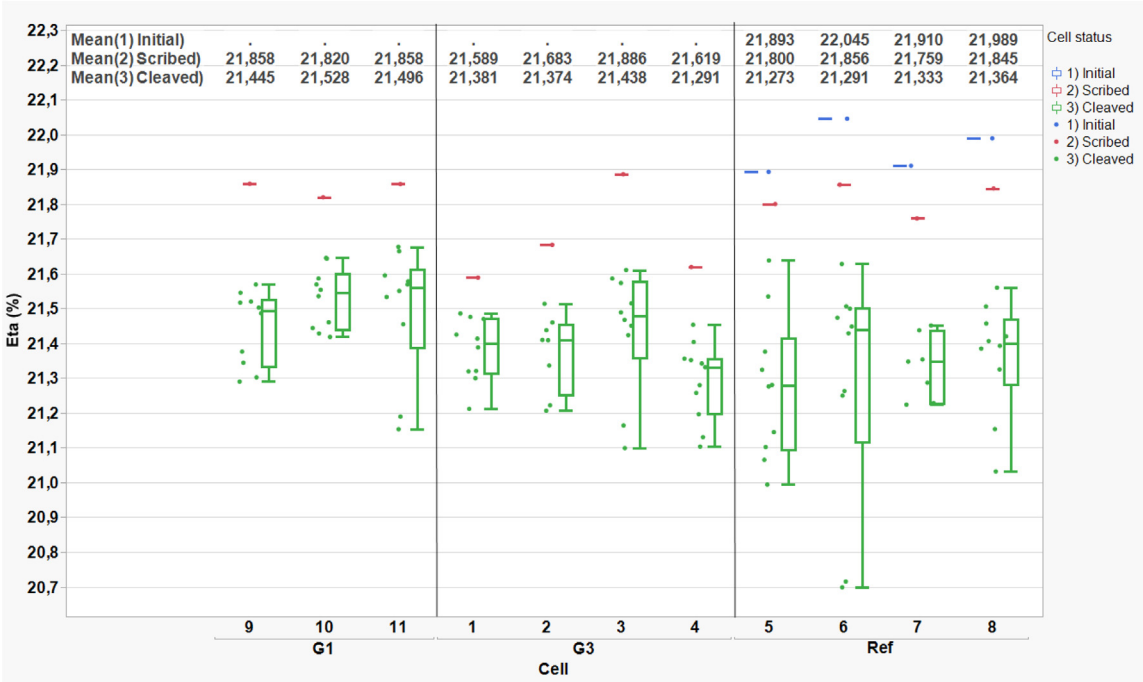

(b)

Fig. 7. (a) V_{OC} values and (b) η values attained by I − V measurements of the cells at initial, scribed and cleaved states.

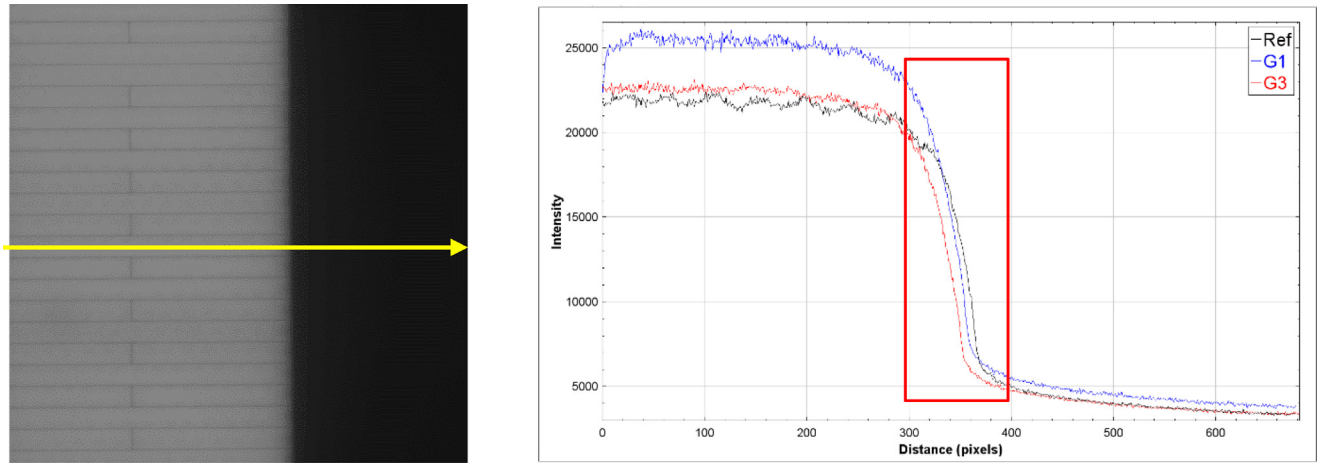

Fig. 8. PL image of the cleaved cell from group 1 under 1-sun illumination, along with the intensity graph.

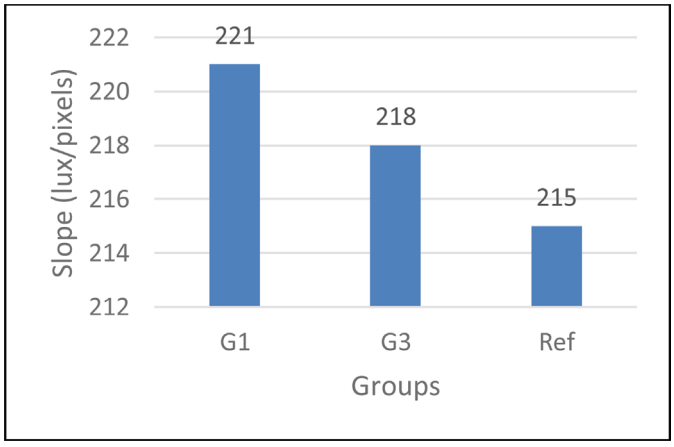

Fig. 9. Slope values for different groups at 1 sun illumination.

Figure 10 shows the LSM images of cell edge from reference, group 1 and group 3. In comparison to the reference cell, cells from group 1 and group 3 have some aluminium filings in the laser groove, although the grooves are not completely filled. The groups doped with aluminium have a lower arithmetical mean roughness value R_a in comparison to reference. Also, it was observed that the depth of the laser groove for G1 and G3 groups is slightly high compared to the reference.

Overall, from this experiment it can be concluded that group 1 cells which were scribed before metallization and then got aluminium doping performed better than the reference cells. An increase in open-circuit voltage and efficiency could be observed for group 1. V_{OC} is increased by $\Delta V_{OC} = +2$ mV whereas η is increased by $\Delta\eta = +0.2\%$. Additionally, PL results also supported the results of IV measurements, with group 1 having better performance in comparison to the reference. LSM results also show some partial filling of aluminium in the laser groove. In conclusion, functionality of this method could be demonstrated which shows a passivation effect on the cell edges and an improvement in η and slight increase in V_{OC} of the cleaved cells.

5 Conclusion

This article introduces two different approaches for passivating the laser separated PERC solar cells. The first method is 'Laser scribing and simultaneous Al doping'. The method uses two steps for scribing. The first scribe melts the aluminium while the second scribe follows the standard recipe for cutting. Different variations of the laser parameters were tested for melting aluminium. The cells, which were only scribed using the standard recipe were taken as the reference cells. There is a drop in the pFF by 1.8% (ΔpFF = − 1.8%) from the host wafer to the separated state for the reference cell. This method increases the pFF of the cleaved cells by $+0.2$–$0.4\%_{abs}$ in comparison to the reference cleaved cells. An improvement in V_{OC} or other cell parameters could not be detected.

The second method is 'Laser scribing and subsequent Al doping.' Here the cells are scribed prior to metallization and then metallized by screen printing, followed by firing. Different variations of the laser scribes, in order to increase the width or depth of the laser groove were tested. The idea behind this technique is to fill the laser grooves with aluminium in order to obtain an edge doped with aluminium after breaking these cells. The cells with no laser scribing before metallization, which followed the standard processing steps were used as reference cells. This method shows an improvement in the open-circuit voltage by $+2$ mV and an increase in efficiency by $+0.2\%_{abs}$. The I–V results were also supported by PL measurements for both the methods.

In summary, this research demonstrated the functionality of both the proposed edge passivation methods. An improvement in some of the I–V parameters of the cell could be observed. The implementation of these methods into industrial PERC production lines is achievable without additional cost. For method 1 nothing has to be changed besides the laser scribing process, while method 2 needs a restructuring of the processes and the mechanical yield could be affected as the already scribed cells have to pass screen printing, firing and cell testing, which could increase the wafer breakage rate.

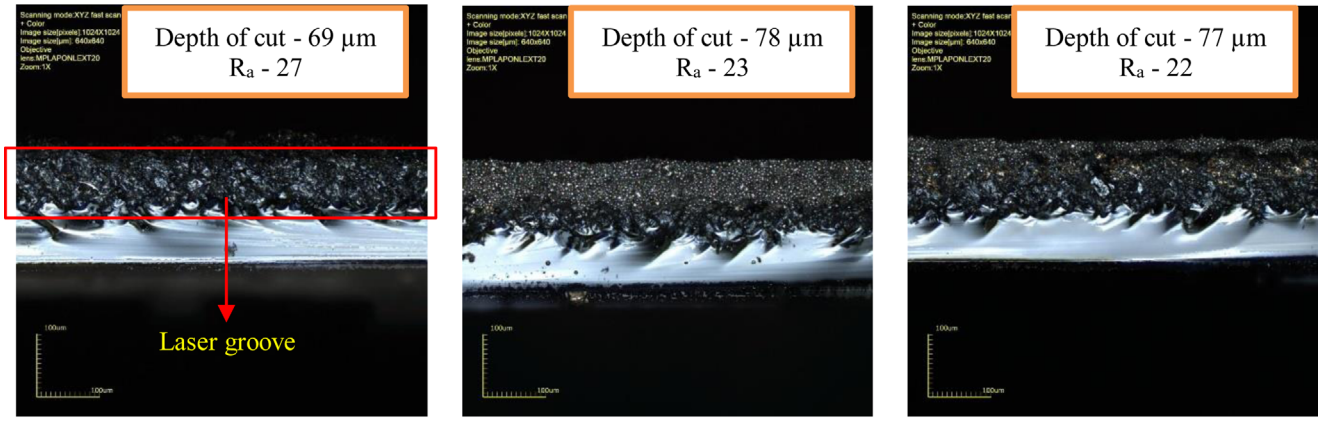

(a) (b) (c)

Fig. 10. LSM images of cell edge, their depth of cut and their corresponding roughness value R_a (inset) from (a) reference group, (b) group 1 and (c) group 3.

Funding

This work is supported by the German Federal Ministry for Economic Affairs and Climate Action (BMWK) as part of the BIG project with funding reference numbers 03EE1116A.

Conflicts of interest

The authors have nothing to disclose.

Data availability statement

The data for the IV results could be provided on request.

Author contribution statement

Conceptualization: Daniel Tune, Dominik Rudolph, Akash Thukaram; methodology: Akash Thukaram, Daniel Tune, Dominik Rudolph; formal analysis: Akash Thukaram, Dominik Rudolph, Daniel Tune, Andreas Halm; investigation: Akash Thukaram, Dominik Rudolph, Daniel Tune, Andreas Halm; experimentation: Akash Thukaram, Dominik Rudolph, writing: Akash Thukaram; supervision: Dominik Rudolph, Daniel Tune, Andreas Halm; writing, review and editing: Akash Thukaram, Dominik Rudolph, Daniel Tune; All authors have read and agreed to the published version of the manuscript.

References

1. 2022 ITRPV Roadmap, Available at: https://www.vdma.org/international-technology-roadmap-photovoltaic
2. J. Schneider, S. Schoenfelder, S. Dietrich, M. Turek, Solar module with half size solar cells, in *Proc. 29th Eur. PVSolar Energy Conf. Exhib., Amsterdam, The Netherlands* (2014), pp. 185–189
3. N. Wöhrle, E. Lohmüller, M. Mittag, A. Moldovan, P. Baliozian, T. Fellmeth, K. Krauss, A. Kraft, R. Preu, Solar cell demand for bifacial and singulated-cell module architectures, Photovolt. Int. **36**, 48 (2017)
4. M. Chiodetti, J. Dupuis, D. Boublil, K. Radouane, P. Dupeyrat, Half-cell module behaviour and its impact on the yield of a PV plant, in *36th European Photovoltaic Solar Energy Conference and Exhibition* (2019) pp. 1444–1448 https://doi.org/10.4229/EUPVSEC20192019-5DO.3.3
5. H. Stolzenburg, A. Fell, F. Schindler, W. Kwapil, A. Richter, P. Baliozian, M.C. Schubert, Edge recombination analysis of silicon solar cells using photoluminescence measurements, AIP Conf. Proc. **2147**, 020017 (2019)
6. A. Münzer, P. Baliozian, K. Ahmed, A. Nair, E. Lohmüller, T. Fellmeth, A. Spribille, R. Preu et al., Laser-assisted separation processes for bifacial pSPEER Shingle solar cells, in *37th European Photovoltaic Solar Energy Conference and Exhibition* (2020) Vol. 7, p. 11. https://doi.org/10.4229/EUPVSEC20202020-2CV.1.51
7. J. Röth, K. Kaufmann, S. Eiternick, C. Belgardt, M. Grimm, N. Bernhard et al., A comparison of different laser separation methods for half cell production, Proc. Am. Math. Soc. **112**, 605 (1991) https://doi.org/10.1090/S0002-9939-1991-1052871-0
8. O. Haupt, Laser dicing of silicon: comparison of ablation mechanisms with a novel technology of thermally induced stress, J. Laser Micro Nanoeng. **3**, 135 (2008) https://doi.org/10.2961/jlmn.2008.03.0002
9. D. Perrottet, S. Green, B. Richerzhagen, Clean dicing of compound semiconductors using the water-jet guided laser technology, in *The 17th Annual SEMI/IEEE ASMC 2006 Conference, Boston, MA* (2006), pp. 233–236
10. P.C. Verburg, G. Roemer, G. Knippels, J. Betz, A. Veld, Experimental validation of model for pulsed-laser-induced subsurface modifications in Si, Appl. Phys. A **114**, 1135 (2014)
11. M. Hermle, J. Dicker, W. Warta, S.W. Glunz, G. Willeke, Analysis of edge recombination for high-efficiency solar cells at low illumination densities, in *3rd World Conference on Photovoltaic Energy Conversion, 2003, Osaka, Japan* (2003), Vol. 2 pp. 1009–1012

12. W.P. Mulligan, A. Terao, D.D. Smith, P.J. Verlinden, R.M. Swanson, Development of chip-size silicon solar cells, in *Conference Record of the Twenty-Eighth IEEE Photovoltaic Specialists Conference – 2000 (Cat. No.00CH37036), Anchorage, AK, USA* (2000), pp. 158–163
13. P.P. Altermatt, G. Heiser, M.A. Green, Numerical quantification and minimization of perimeter losses in high-efficiency silicon solar cells, Prog. Photovolt.: Res. Appl. **4**, 355 (1996)
14. P. Baliozian, M. Al-Akash, E. Lohmüller, A. Richter, T. Fellmeth, A. Münzer, N. Wöhrle, P. Saint-Cast, H. Stolzenburg, A. Spribille, R. Preu, Postmetallization "passivated edge technology" for separated silicon solar cells, IEEE J. Photovolt. **10**, 390 (2020). https://doi.org/10.1109/JPHOTOV.2019.2959946
15. D. Tune, F. Buchholz, A. Halm, Measuring and mitigating edge recombination in modules employing cut cells, in *Proceedings of the 37th European Photovoltaic Solar Energy Conference and Exhibition* (2020), pp. 322–328
16. E. Lohmüller, P. Baliozian, L. Gutmann, L. Kniffki, V. Beladiya, J. Geng, L. Wang, R. Dunbar, A. Lepert, M. Hofmann, A. Richter, J.D. Huyeng, Thermal laser separation and high-throughput layer deposition for edge passivation for TOPCon shingle solar cells, Sol. Energy Mater. Sol. Cells **258**, 112419 (2023)
17. A. Münzer, P. Baliozian, A. Steinmetz, T. Geipel, S. Pingel, A. Richter, S. Roder, E. Lohmüller, A. Spribille, R. Preu, Post-separation processing for silicon heterojunction half solar cells with passivated edges, IEEE J. Photovolt. **11**, 1343 (2021) https://doi.org/10.1109/JPHOTOV.2021.3099732
18. F. Gerenton, S. Harrison, J. Eymard, P. Lefillastre, R. Varache, V. Nguyen, D. Munoz, C. Roux, Silicon heterojunction and half-cell configuration: optimization path for increased module power, in *2019 IEEE 46th Photovoltaic Specialists Conference (PVSC)*. https://doi.org/10.1109/PVSC40753.2019.8981179
19. P. Baliozian, E. Lohmüller, T. Fellmeth, N. Wöhrle, A. Krieg, R. Preu, Bifacial shingle solar cells on p-type Cz-Si (pSPEER), AIP Conf. Proc. **1999**, 110002 (2018)

Cite this article as: Akash Thukaram, Dominik Rudolph, Andreas Halm, Daniel Tune, New approaches to edge passivation of laser cut PERC solar cells, EPJ Photovoltaics **15**, 24 (2024)